Journal of King Saud University – Engineering Sciences (2012) **24**, 25–33

King Saud University

Journal of King Saud University – Engineering Sciences

www.ksu.edu.sa
www.sciencedirect.com

ORIGINAL ARTICLE

Strengthening of concrete slab-column connections using CFRP strips

Khaled Soudki [a,1], Ahmed K. El-Sayed [b,*,2], Tim Vanzwol [c]

[a] *Department of Civil and Environmental Engineering, University of Waterloo, 200 University Avenue West, Waterloo, Ontario, Canada*
[b] *Center of Excellence for Concrete Research & Testing, Department of Civil Engineering, King Saud University, P.O. Box 800, Riyadh 11421, Saudi Arabia*
[c] *Department of Civil and Environmental Engineering, University of Waterloo, 200 University Avenue West, Waterloo, Ontario, Canada*

Received 27 September 2010; accepted 4 May 2011
Available online 28 August 2011

KEYWORDS

Punching shear;
Concrete slabs;
Carbon fiber-reinforced polymer;
Strengthening

Abstract This paper presents experimental data and results on the effect of externally bonded carbon fiber-reinforced polymer (CFRP) strips on the punching shear of interior slab-column connections. A total of six square slabs with a concentric column were constructed with overall dimensions of 1220 mm by 1220 mm and 100 mm thick slab and 150 × 150 mm column. The test variables were the configuration and amount of CFRP strips externally bonded to the tension face of the slab. The specimens were simply supported along their edges and tested in punching with vertical load applied through the central column. The test results clearly showed that CFRP strengthening leads to significant improvements in the structural behaviour of slab-column connections. The increase in punching capacity of strengthened slabs was up to 29%, while the increase in stiffness was up to 80% compared to the unstrengthened slab. Punching capacities of the test specimens were evaluated using a recently developed model that accounts for both configuration and amount of CFRP strips.

* Corresponding author. Tel.: +966 469 6345; Mobile: +966 0569 483 706.
E-mail address: ahelsayed@ksu.edu.sa (A.K. El-Sayed).
[1] Visiting professor at King Saud University, Saudi Arabia.
[2] Concrete Structures Institute, Housing and Building National Research Centre, Giza, Egypt.

Peer review under responsibility of King Saud University.
doi:10.1016/j.jksues.2011.07.001

The predicted punching capacities using the analytical model were compared with the experimental results, and good agreement was found.

1. Introduction

Flat concrete slabs are a typical form of flooring systems used in a wide range of buildings such as offices, warehouses and parking garages. Flat slabs are directly supported on columns providing more vertical clear space due to the absence of beams. The connection between the slab and the column in this system is generally the most critical part due to its vulnerability to punching shear failure. Punching shear failures are very brittle in nature and take place within small deflections. Punching strength in slabs can become insufficient due to several reasons such as change of building use, need of instaling new services which requires openings in the slabs, corrosion of reinforcement, and construction or design errors. Punching shear is characterized by cracking within the slab around the column with a truncated cone-shaped element being displaced. In general, the predicted punching failure load is governed largely by the flexural characteristics of the slab.

Over the past decade, a significant amount of research has dealt with various strengthening techniques for concrete slab-column connections in order to prevent sudden punching shear failure. One of the most common strengthening techniques is based on the use of external reinforcement. Several researchers have investigated different methods to strengthen interior slab-column connections against punching including use of steel plates and bolts (Marzouk and Jiang, 2007; Zhang et al., 2001; Ebead and Marzouk, 2002), transverse prestressed reinforcement (Ghali et al., 1974) and more recently the use of fiber reinforced polymer (FRP) composites externally bonded to the slab tension face (Tan et al., 1996; Harajli and Soudki, 2003; Sharaf et al., 2006). Some of these strengthening methods do provide enough additional strength to the slab, however, they are elaborate, difficult to instal, expensive and aesthetically not pleasing. Strengthening slabs with FRPs is simple, does not require excessive labour and does not change the appearance of the slab. However, there is limited literature on the effectiveness of externally bonded FRP strips in increasing the two-way shear capacity of interior slab-column connections.

Ebead et al. (2002) tested two-way slab-column connections to investigate the effect of using CFRP reinforcement as external strengthening technique against punching shear failure. The test programme consisted of three specimens with dimensions of 1900 mm long, 1900 mm wide, and 150 mm deep with internal reinforcement ratio of 1.0%. The specimens had square column stubs (250 mm long × 250 mm wide). Two specimens were strengthened with different configurations of 100-mm-wide CFRP strips. The CFRP-strengthened specimens had an average increase of 9% in the ultimate load capacity over the unstrengthened specimen.

Harajli and Soudki (2003) evaluated experimentally the punching shear capacity of interior slab-column connections strengthened by CFRP sheets. Sixteen square (670 × 670 mm) slab-column connections with different slab thicknesses (55 and 75 mm) and reinforcement ratios (1% and 1.5%) were tested. The CFRP sheets were bonded to the tension face of the specimens in two perpendicular directions parallel to the internal steel reinforcement. The test results indicated that the increase in punching capacity of the strengthened connections was up to 45% over that of the control.

Sharaf et al. (2006) tested a total of six full-scale slab-column connections to study the effect of externally bonded CFRP strips on the punching shear capacity. The slabs measured 2000 mm long, 2000 mm wide, and 150 mm thick and were cast monolithically with a column of 200 mm square cross-section that extended 200 mm from the top and bottom slab surfaces. The main variables were the CFRP strengthening amount and configuration. The findings of this study indicated that the CFRP strengthening resulted in delaying the initiation and controlling of flexural cracks in the slabs. In addition, the measured increase in punching load of the strengthened slabs was up to 16% greater than that of the control slab.

Punching shear of a concrete slab is provided by four different mechanisms. These mechanisms include the contribution from uncracked concrete above the neutral axis, aggregate interlock, dowel action, and residual tensile stresses across the inclined cracks. The bottom steel reinforcement is one of the design parameters known to influence the punching shear capacity of concrete slabs (Ebead et al., 2002). Increasing the reinforcement ratio of steel results in cracks with lower widths and depths. Lower crack width increases the contribution of aggregate interlock as well as the contribution of residual tensile stresses to the punching capacity. On the other hand, shallow depth of the cracks increases the contribution of uncracked concrete to punching capacity. Thus, increasing the bottom steel reinforcement ratio increases the overall punching capacity. It is expected that adding FRP reinforcement to the tension face of concrete slabs will increase the punching capacity as if increasing the bottom steel reinforcement ratio.

The main objective of this study is to investigate the effectiveness of using CFRP strips to strengthen reinforced concrete slabs against punching shear failure. This paper presents the experimental results of the study and a comparison of the test data with an analytical model.

2. Experimental investigation

The experimental programme described in this paper consisted of punching shear tests on six reinforced concrete slabs. Five among the six slabs were strengthened with externally bonded CFRP strips. The primary test variable was the configuration and layout of the CFRP reinforcement.

2.1. Material properties

The slabs were constructed using ready-mixed concrete provided by a local supplier. The average 28-day compressive

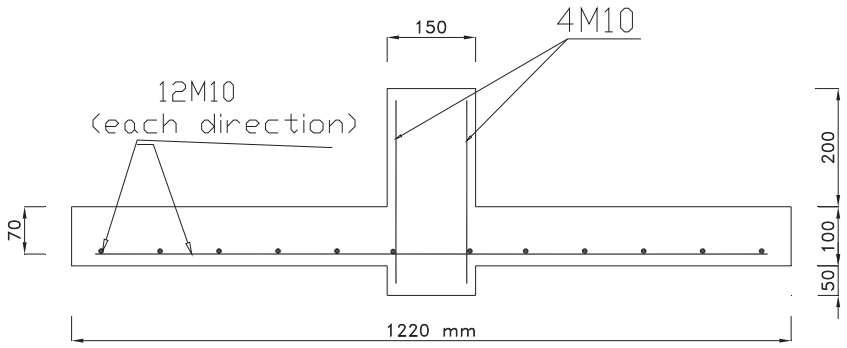

Figure 1 Test specimen dimensions and reinforcement layout.

Table 1 Test matrix.

Slab specimen	Number of CFRP strips	Description of strengthening configuration
S	–	Control; no strengthening
S-4-O-O	4	Orthogonal; offset column face
S-4-O-A	4	Orthogonal; adjacent to column face
S-4-S-O	4	Skewed; offset column face
S-4-S-A	4	Skewed; adjacent to column edge
S-8-O-AO	8	Orthogonal; adjacent to and offset column face

strength of concrete was 25.8 MPa based on testing standard concrete cylinders. Deformed steel bars No. 10M (d_b = 11.3 mm) were used in reinforcing the concrete slabs. The average yield strength of the steel bars was 440 MPa obtained from unaxial tension tests. The strips used to strengthen the concrete slabs were Sika CarboDur S1012 unidirectional CFRP. The strips were 100 mm wide and 1.2 mm in thickness, with a cross-sectional area of 120 mm^2. At a density of only 1.6 g/cm^3, the CFRP material has a very high strength to weight ratio. The strips have a specified tensile strength of 2400 MPa and a modulus of elasticity of 155 GPa, as provided by the manufacturer. To bond the CFRP strips to the concrete surface, Sikadur

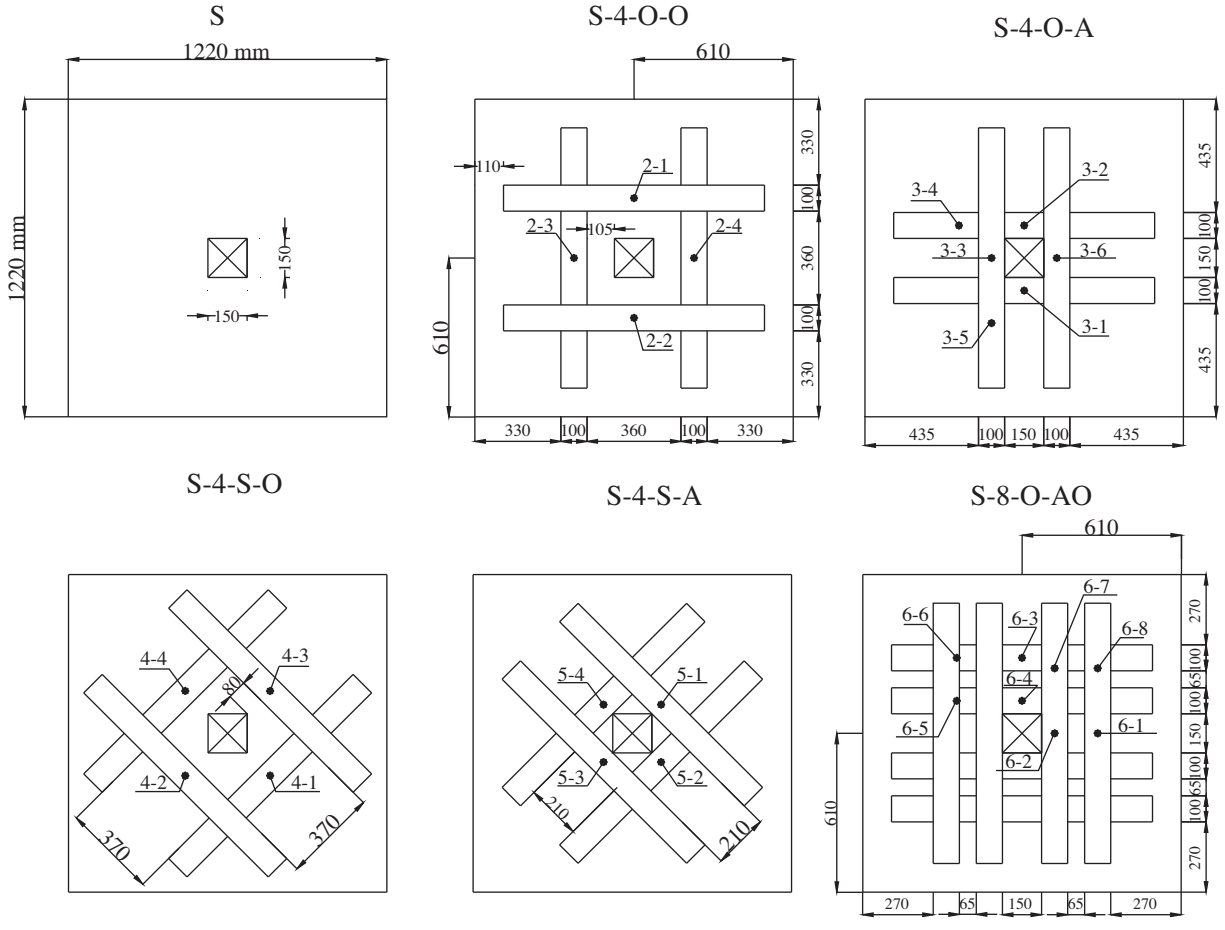

Figure 2 CFRP strengthening schemes.

30 was used, which is a high-modulus high-strength two-component epoxy product.

2.2. Test specimens

Six reinforced concrete interior slab-column connections were constructed with the same geometrical configuration and steel reinforcement details. The overall slab dimensions were 1220 mm by 1220 mm and 100 mm thick. Each slab was reinforced by one bottom layer of No. 10M steel bars, spaced 100 mm c/c, in each direction. A central column stub (150 mm × 150 mm) was cast monolithic with the slab and extended from both the compression and tension face of the slab to simulate as close as possible conditions and construction limitations that would exist in strengthening actual interior slab-column connection. No. 10M vertical steel bars were placed in each corner of the column stub. Along the slab sides, an average concrete cover of 40 mm was ensured. Clear concrete cover from the bottom layer of reinforcement to the underside of the slab measured 20 mm. Fig. 1 shows the typical dimensions and steel reinforcement layout of the test specimens.

The six specimens included one specimen unstrengthened to serve as a control specimen. The other five were externally strengthened using different configurations of CFRP strips bonded to the tension face of the slab. Table 1 gives the description of CFRP strips and specimen designation. The designation of the slabs uses the first letter S standing for slab and the numbers 4 and 8 referring to the number of CFRP strips. The second letter O or S refers to the scheme of CFRP strips: orthogonal or skewed, respectively. The third letter, O, A, or AO refers to the location of CFRP strips to the column: offset, adjacent, or adjacent and offset, respectively. Fig. 2 shows the CFRP strengthening schemes used in this study.

2.3. Strengthening procedure

The CFRP strips were cut into 1 m long for strengthening the concrete slabs. The CFRP strips were placed in an orthogonal or skew orientation as shown in Fig. 2. The strips were bonded at the column face or offset by a distance 1.5d from column face (d = distance from compression fibre to tension steel centroid) for slab S-4-O-O and 1.15d from column corner for slab S-4-S-O. One slab (Slab S-8-O-AO) was strengthened with two rows of CFRP strips placed in two perpendicular directions. Special consideration was given to the surface preparation before bonding the CFRP strips to the concrete surface. Sandblasting was employed to remove the weak surface layer from the concrete slabs and then the surface was cleaned with a high-pressure air jet and the CFRP strips was bonded to the concrete surface using the epoxy adhesive. The epoxy adhesive was first applied to marked locations on the concrete surface with a trowel. Additional adhesive was applied at points where strips would overlap. Then, the strips were pressed onto the

Figure 3 Test setup.

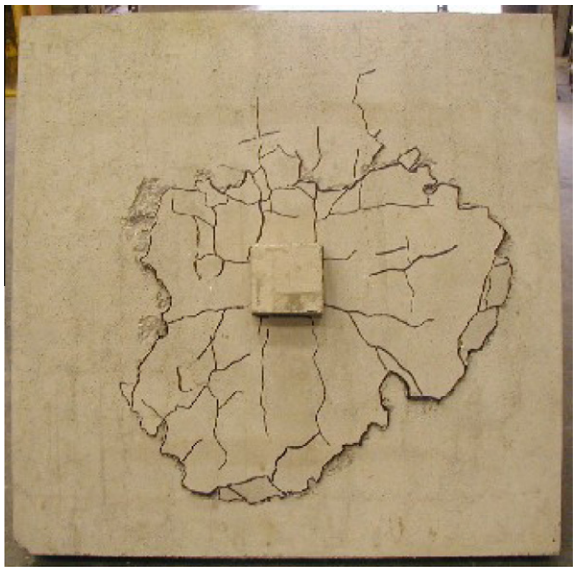

Figure 4 Punching shear failure cracks on slab S (bottom face).

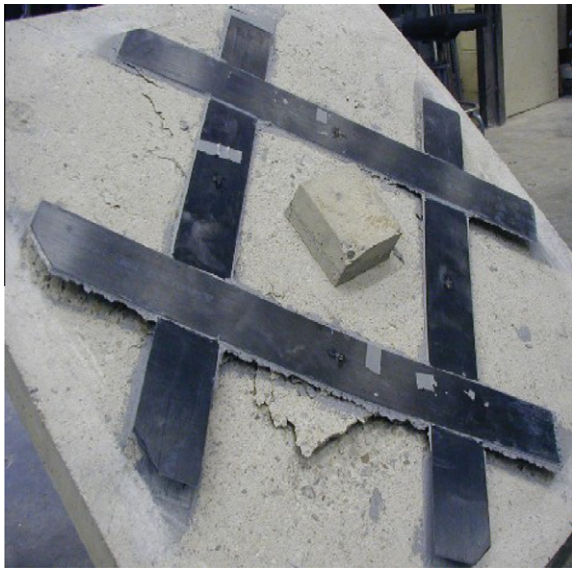

Figure 5 Punching shear failure cracks on slab S-4-S-O (bottom face).

Table 2 Summary of test results.

Slab specimen	Ultimate load P_u (kN)	Ratio $P_u/P_{u(control)}$	% Increase above control	Deflection at ultimate load (mm)	Post-cracking stiffness (kN/mm)
S	160.3	1.00	0	14.4	12.1
S-4-O-O	181.0	1.129	12.9	10.3	18.0
S-4-O-A	163.8	1.022	2.2	8.1	20.5
S-4-S-O	206.9	1.291	29.1	10.7	19.5
S-4-S-A	173.7	1.084	8.4	9.0	19.5
S-8-O-AO	192.9	1.203	20.3	8.9	21.7

concrete substrate using a small roller. Excess adhesive was squeezed out the sides and removed; this ensured that any trapped air was removed. After the entire application process was complete the adhesive ranged between 2 and 3 mm in overall layer thickness.

2.4. Test setup and instrumentation

Fig. 3 shows the test set-up. The test specimens were mounted on a steel frame and were simply supported along all four edges. The specimens were loaded centrally through the column stub with monotonically increasing load until failure. The load was applied at a rate of 15 kN/min using a servo-controlled hydraulic actuator. Test measurements included the magnitude of the applied load, deflection of the slab at the column location, and strains in the CFRP strips. Deflection at the centre of the slab was measured using a linear variable differential transducer (LVDT) placed underneath the centre of the bottom column stub. The strains in the CFRP strips were measured using electrical resistance strain gages attached at mid width of the strips at different locations as shown in Fig. 2. Based on the number and configuration of CFRP strips bonded to the slab tension face, four to eight strain gages were mounted on the CFRP strips. All instrumentation measurements were recorded during testing using a computer-based data acquisition system. At the end of each test, the angle at which the shear cracks propagated away from the column faces was measured and the mode of failure for each specimen was examined.

3. Test results and discussion

3.1. Ultimate load and modes of failure

The control slab, slab S, exhibited flexural cracks that originated near the centre of the column stub and propagated towards the edges of the slab. Punching shear was the primary reason for failure within this slab. Once the slab reached its ultimate load capacity, it failed suddenly due to punching shear. This is characterized by a sharp drop in the load versus deflection plot immediately after the ultimate load is reached. Fig. 4 shows by photograph the mode of failure of slab S. The punching shear failure plane can be seen around the column on the underside of the slab. Distances from the face of the column to the punching shear failure plane ranged from 130 mm to 420 mm. The average distance was approximately 280 mm or 4*d*. This is significantly greater than 170 mm calculated if the shear failure plane is assumed to act at a 30° angle.

For the CFRP strengthened specimens, the strips at failure load debonded transversally near the shear crack as a result of the transverse movement of concrete on either sides of the crack due to punching failure. The mode of failure of slabs strengthened with four CFRP strips was characterized first by yielding of the internal steel reinforcement. Concurrently, some of the CFRP strips debonded from the concrete surface. As the strips pulled away from the specimen, the concrete cover was also removed with the strengthening strips; this was a result of tension failure within the concrete. Therefore, although the strips were pulled away from the underside of the concrete slab, it was not a result of epoxy or concrete-epoxy bond failure. Finally, punching shear failure was experienced at the ultimate load of the specimen. Strips debonded from the slab as the truncated concrete cone was pushed through the slab. The shear cracking appeared to be an average of 200–300 mm (2.9*d* – 4.3*d*) from the column face, i.e., similar to control specimen. Fig. 5 illustrates the mode of failure of one of the strengthened slabs as a typical (slab S-4-S-O). Slab S-8-O-AO with eight CFRP strips experienced the same mode of failure as the previous four strengthened slabs. However, due to the large amount of strengthening, most of the punching shear cracks were concealed under the CFRP strips. Some of the visible punching shear cracks were measured at an average distance of 150 mm from the column face.

Table 2 gives a summary of the test results. The control specimen experienced the lowest punching load of 160.3 kN. All the strengthened specimens had higher punching loads than the control specimen as shown in Fig. 6 and given in Table 2. The increase in punching shear capacity was compared with the control slab. Overall, slab S-4-S-O had the greatest increase in punching shear capacity with 29.1% increase over the control slab. Slab S-8-O-AO also exhibited a significant increase in punching shear capacity with a 20.3% increase.

Comparing the different CFRP strips arrangements, it can be noted that the skewed strengthening arrangement gave

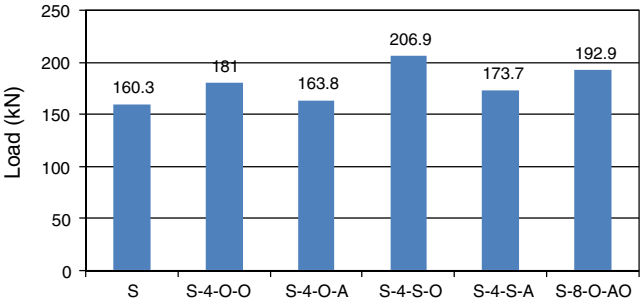

Figure 6 Measured ultimate loads supported by slabs.

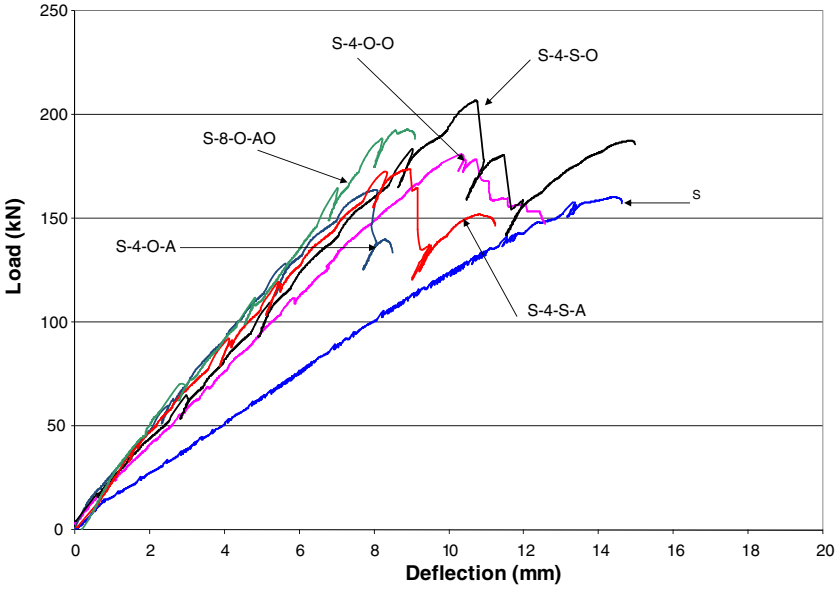

Figure 7 Load–deflection relationship.

higher punching load increase compared to the orthogonal arrangement. Slabs S-4-S-O and S-4-S-A with skewed strips had 29.1% and 8.4% increase in the punching load over the control slab, respectively; while the counterparts with orthogonal strips had 12.9% and 2.2% increase in the punching load. This may be attributed to the fact that the strips of the skewed strengthening pattern were orientated in a different manner compared to the interior reinforcement which orientated in orthogonal pattern. Taking into account that punching shear cracks are spread in radial pattern, this makes the skewed CFRP strips with orthogonal interior reinforcement more efficient in restricting the growth of these cracks.

Considering the location of the CFRP strips from the column face, it can be noted that the strips place offset the column face produced relatively higher increase in punching capacity. For slabs with orthogonal strengthening pattern, slab S-4-O-O with offset strips experienced higher load compared to slab S-4-O-A with strips placed adjacent to the column face. Similarly and for slabs with skewed strengthening pattern, slab S-4-S-O with offset strips experienced increase in punching strength than that of slab S-4-S-A with strips placed adjacent to the column face.

Slab S-8-O-AO with eight strips place near and offset the column face in orthogonal pattern experienced higher strength compared to the slabs S-4-O-O and S-4-O-A with four strips of orthogonal pattern. However, the increase in punching capacity of slab S-8-O-AO was less than that of slab S-4-S-O with four strips in skewed pattern. Based on these test results and the previous discussion, it can be concluded that the most effective configuration was the skewed strip arrangement offset the column face.

3.2. Load deflection behaviour

Fig. 7 compares the load versus deflection plots for all slab specimens. The load–deflection response was bilinear up to the ultimate load and can be divided into uncracked and cracked stages. All specimens showed the same behaviour in the uncracked stage, while the post-cracking behaviour appeared to be different. From Fig. 7 and Table 2, it can be seen that the overall post-cracking stiffness of the CFRP strengthened slabs are considerably greater than the control slab. The stiffness was calculated as the slope of the load-deflection curve.

Comparing the effect of the location of the CFRP strips related to the column face, it can be noted that slab S-4-O-A with orthogonal strengthening located adjacent to the column face, showed higher post-cracking stiffness compared to slab S-4-O-O with orthogonal strengthening offset the column face. This result indicates that strengthening placed near

Table 3 Measured CFRP strain.

Slab specimen	Location of strain gauge	CFRP strain at ultimate load (με)
S-4-O-O	Centre – top strips	3062
	Centre – bottom strips	2615
S-4-O-A	Centre – top strips	2481
	Centre – bottom strips	2811
	250 mm offset – top strips	2017
	250 mm offset – bottom strips	1945
S-4-S-O	Centre – top strips	3554
	Centre – bottom strips	3533
S-4-S-A	Centre – top strips	2851
	Centre – bottom strips	2773
S-8-O-AO	Centre – top/outer strips	1803
	Centre – top/inner strips	2254
	Centre – bottom/outer strips	2894
	Centre – bottom/inner strips	2866
	250 mm offset – top/outer strips	1330
	250 mm offset – top/inner strips	1728
	250 mm offset – bottom/outer strips	1865
	250 mm offset – bottom/inner strips	2268

the column face produces relatively higher stiffness values than strengthening offset from the column. However, this finding is not supported by the results of slabs with skewed strengthening pattern. Slabs S-4-S-O and S-4-S-A exhibited very similar stiffness characteristics as given in Table 2 despite the difference of the location of the CFRP strips related to the column face in the two slabs. Slab S-8-O-AO, containing the most amount of strengthening, produced the highest post-cracking stiffness of 21.7 kN/mm with about 80% increase in stiffness in comparison to that of the control specimen.

With regard to the ultimate deflection, the control specimen had the highest deflection value at the corresponding ultimate load. Deflection values at the ultimate loads of the strengthened specimens were between 56% and 74% of the deflection value of the control specimen due to the observed stiffening effect of CFRP strips.

3.3. FRP strains

In general the load versus CFRP strain relationship was bilinear for all strengthened slab specimens until punching shear failure occurred. Table 3 summarizes maximum strain measured. In the table, all the strain gage locations are listed in addition to the maximum strains measured at the ultimate load capacities. From Table 3, the top overlapping CFRP strips experienced a higher strain than the bottom strips for slabs S-4-O-O, S-4-S-O, and S-4-S-A. These top strips were also located further away from the slab surface. On the other hand, the bottom strips (closer to the slab surface) of slabs S-4-O-A and S-8-O-AO experienced higher strains. Since the strips in these specimens were spaced closer together, they would lead to more load sharing between the strips and thus higher strains in these lower strips. Also, it is evident from Table 3 that the strain decreases away from the centre of the slabs (slabs S-4-O-A and S-8-O-AO). Strains in the strips of slab S-4-S-O were very similar with the highest strains measured compared to all of the other strengthened specimens because this slab experienced the maximum ultimate load. The maximum measured strain was 3554 με which represents 23% of the capacity of CFRP strip (15,500 με).

Some of the instrumented strips of slabs S-4-O-A and S-8-O-AO were instrumented with two strain gauges at different locations which allow calculating the strain gradient. The strain gradient in CFRP strips at ultimate load ranged between 1.42 and 3.17 με/mm, which is much less than that required to cause peeling at 88 με/mm as per Miller and Nanni (1999). Thus peeling of the strips is not a concern in this particular strengthening application as also observed by Ospina et al. (2001).

4. Calculated punching capacities

An analytical model has been recently developed by Harajli and Soudki (2003) to predict the punching shear capacity of FRP strengthened slab-column connections. This model is based on the fact that increasing the flexural capacity of the slabs increases the punching capacity as well. To incorporate the effect of the external FRP strips on the flexural capacity, the average moment capacity per unit width (m) of the FRP strengthened slab was derived using the conventional force and moment equilibrium requirements and strain compatibility across the depth of the slab section as follows:

$$m = \rho_s f_y d^2 \left[1 - 0.59\left(\rho_s \frac{f_y}{f'_c} + \rho_f \frac{k_v f_{fu} h/d}{f'_c}\right)\right] + \rho_f k_v f_{fu} h^2 \left[1 - 0.59\left(\rho_s \frac{f_y d/h}{f'_c} + \rho_f \frac{k_v f_{fu}}{f'_c}\right)\right] \quad (1)$$

where

$$\rho_s = \frac{A_s}{wd}, \quad \rho_f = \frac{A_{frp}}{wh} \quad (2)$$

in which ρ_s and ρ_f are the reinforcement ratios of the internal steel and external CFRP reinforcement, respectively; A_s is the cross-sectional area of the steel used per slab panel of width w; A_{frp} is the cross-sectional area of CFRP strips; h is overall height of the slab section; d is depth of tension steel reinforcement; f_y is yield stress of reinforcing steel; f'_c is the concrete compressive strength; and k_v is efficiency factor which represents the ratio of stress developed in CFRP strips at ultimate strength capacity of the specimens to the ultimate strength f_{fu} of the strips.

The factor k_v in Eq. (1) accounts for possible delamination failure from the concrete (ISIS Canada, 2001), and is given as:

$$k_v = \frac{K_1 K_2 L_e}{11,900\varepsilon_{fu}} \leqslant 0.75 \quad (3)$$

The active bond length, L_e, is the length over which the bond stress is maintained. It is given as:

$$L_e = \frac{25,350}{(t_f E_f)^{0.58}} \quad (4)$$

where t_f and E_f represent the CFRP strip thickness and modulus of elasticity, respectively. The factors K_1 and K_2 which account for the concrete strength and wrapping scheme are given as:

$$K_1 = \left(\frac{f'_c}{27}\right)^{2/3} \quad (5)$$

$$K_2 = \frac{L_f - 2L_e}{L_f} \quad (6)$$

where L_f is the slab dimension in the direction of FRP strips.

Sharaf et al. (2006) refined this model to include the effects of strengthening configuration, amount and spacing of FRP strips by modifying the calculation of the effective area of FRP strips as follows:

$$A_{frp} = \sum_{i=1}^{n} \frac{\eta}{\zeta} b_{fi} t_{fi} \quad (7)$$

in which, η is a factor that represents the effect of FRP fibre orientation and is given as:

$$\eta = \Delta \cos\theta \quad (8)$$

where θ is the orientation of FRP strips relative to steel bars and Δ is taken 1 for orthogonal FRP strips and 2 for skewed FRP strips.

The factor ς in Eq. (7) accounts for the effect of FRP strips locations relative to the column face or corner, the spacing

Table 4 Calculated punching shear capacity of the CFRP strengthened slabs (Eqs. (1)–(11)).

Slab specimen	d (mm)	L_f (mm)	n	η	ς	A_{frp} (mm^2)	ρ_{frp}	L_e (mm)	K_1	K_1	K_2	m (kN m/m)	P_{flex}	$P_{u\ calc}$
S-4-O-O	70	1150	2	1	0.65	369	0.0032	22.3	0.97	0.96	0.113	31.8	249	182.6
S-4-O-A	70	1150	2	1	2.0	120	0.001	22.3	0.97	0.96	0.113	27.3	214	174.7
S-4-S-O	70	1150	2	1.41	0.77	439	0.0038	22.3	0.97	0.96	0.113	33.1	259	184.4
S-4-S-A	70	1150	2	1.41	2.0	169	0.0015	22.3	0.97	0.96	0.113	28.2	221	176.4
S-8-O-AO	70	1150	4	1	1.23	195	0.0017	22.3	0.97	0.96	0.113	28.7	224	177.3

Table 5 Comparison of experimental and calculated punching capacities of the CFRP strengthened slabs.

Slab specimen	$P_{u\ test}$ (kN)	Analytical model (Eqs. (1)–(11))		ACI 318-08 (Eq. (12))		CSA-A23.1.3-04 (Eq. (13))	
		$P_{u\ calc}$	$P_{u\ test}/P_{u\ calc}$	$P_{u\ calc}$	$P_{u\ test}/P_{u\ calc}$	$P_{u\ calc}$	$P_{u\ test}/P_{u\ calc}$
S-4-O-O	181	182.6	0.99	103.3	1.75	118.9	1.52
S-4-O-A	163.8	174.7	0.94	103.3	1.59	118.9	1.38
S-4-S-O	206.9	184.4	1.12	103.3	2.0	118.9	1.74
S-4-S-A	173.7	176.4	0.98	103.3	1.68	118.9	1.46
S-8-O-AO	192.9	177.3	1.09	103.3	1.87	118.9	1.62
Average			1.02		1.78		1.54
Standard deviation			0.08		0.16		0.14
Coefficient of variation (%)			7.5		9.1		9.1

between the FRP strips, and the number of the FRP strips. This factor is calculated as follows:

$$\zeta = \frac{\sum_{i=1}^{n} \frac{b_{fi}}{s_i}}{n} \tag{9}$$

where b_f is the width of FRP strip, s is the distance from centre of each FRP strip to column face, and n is the total number of FRP strips per slab width.

Once the average moment capacity per unit width (m) of the FRP strengthened slab is determined (Eqs. (1)–(9)), the flexural capacity of the slab, P_{flex}, can be calculated based on the yield line analysis as follows (Elstner and Hognestad, 1956):

$$P_{flex} = 8m\left(\frac{1}{1 - r/w} - 3 + 2\sqrt{2}\right) \tag{10}$$

in which r is the side length of a square loaded area or width of a column.

The punching shear strength, P_u, of the strengthened slab is calculated according to the equation proposed by Mowrer and Vanderbilt (1967) as follows:

$$P_u = \frac{0.8(1 + d/r)bd\sqrt{f'_c}}{1 + (0.433bd\sqrt{f'_c}/P_{flex})} \tag{11}$$

where b is perimeter of column or loaded area.

Table 4 presents detailed calculations of the predicted punching shear capacity of the slab specimens tested in the current study according to Eqs. (1)–(11) while these predicted values are compared with the experimental ones as given in Table 5. It can be noted that the analytical model proposed by Harajli and Soudki (2003) and modified by Sharaf et al. (2006) (Eqs. (1)–(11)) provides accurate predictions for the punching capacity of the tested slabs as the average of the ratio $P_{u\ test}/P_{u\ calc}$ is 1.02 with a coefficient of variation of 7.5%.

The experimental results are also compared with the American Concrete Institute (ACI) building code (ACI Committee, 2008) equation and the equation of the Canadian Standards Association (CSA) (CSA, 2004) for interior slab-column connections. The ACI equation for the two-way shear strength is:

$$P_u = \left(0.17 + \frac{0.33}{\beta_c}\right)\sqrt{f'_c}b_o d \leqslant 0.33\sqrt{f'_c}b_o d \tag{12}$$

where β_c is the ratio of the long side to the short side of the column, b_o is the perimeter of the critical section for punching shear taken at a distance of $d/2$ from the periphery of the column.

The CSA equation for two-way shear strength is:

$$P_u = 0.19\left(1 + \frac{2}{\beta_c}\right)\lambda\phi_c\sqrt{f'_c}b_o d \leqslant 0.38\lambda\phi_c\sqrt{f'_c}b_o d \tag{13}$$

where λ is a factor accounting for the concrete density, ϕ_c is a material reduction factor for concrete. Similar to the ACI method, b_o is calculated at the critical section for punching shear which is at a distance of $d/2$ from the periphery of the column.

Table 5 shows that both ACI and CSA equations provide very conservative predictions for the punching shear strength of the tested slabs in comparison to the proposed model by Harajli and Soudki (2003) and modified by Sharaf et al. (2006) (Eqs. (1)–(11)). The average ratio $P_{u\ test}/P_{u\ calc}$ is 1.78 using the ACI equation and 1.54 using the CSA equation compared to 1.02 for the proposed model as given in Table 5. It should be noted that the code equations do not account for the effect of FRP reinforcement and these provisions are not intended for FRP design.

5. Conclusions

The results of experimental investigation on the punching shear behaviour of slab-column connections strengthened in bending with CFRP strips were presented. A total of six square slabs with a concentric column were tested under monotonic loading conditions: five slabs with CFRP strips externally bonded to the tension face and one control slab without CFRP strips. The primary test parameters were the orientation and configuration of CFRP strips. The main findings of this investigation can be summarized as follows:

1. All six slabs failed in punching shear mode. The strengthened slabs experienced higher punching capacity compared with the control slab. The increase in punching capacity was up to 29% due to strengthening with CFRP strips.
2. The strengthened slabs exhibited much stiffer responses and lower deflections than the control slab.
3. Strengthening placed near the columns produced higher stiffness values and strengthening offset from the column face increased the punching capacity.
4. The most efficient configuration for CFRP strips appeared to be the skew orientation away from the perimeter of the column.
5. Increasing the amount of CFRP strips did not significantly increase the capacity of the slabs.
6. The calculated punching shear capacities of the tested slabs using the recently developed analytical model, in which the two-way shear is expressed as a function of the flexural strength of the connection, agree very well with the experimental results.

Acknowledgement

The authors acknowledge the financial support from the Natural Sciences and Engineering Research Council of Canada (NSERC). The authors would like to thank the technical staff in the structures laboratory at the University of Waterloo for their assistance in fabricating and testing the specimens.

References

ACI Committee 318, Building code requirements for structural concrete and commentary, ACI 318-08/ACI 318R-08, American Concrete Institute, Farmington Hills, MI, 2008.

Canadian Standards Association (CSA), Design of Concrete Structures, CAN/CSA-A23.3-04, Rexdale, Ontario, 2004.

Ebead, U., Marzouk, H., 2002. Strengthening of two-way slabs using steel plates. ACI Structural Journal 99 (1), 23–31.

Ebead, U., 2002. Strengthening of reinforced concrete two-way slab, PhD thesis, Memorial University of Newfoundland, St. John's, Newfoundland, Canada, p. 231.

Elstner, R.C., Hognestad, E., 1956. Shearin strength of reinforced concrete slabs. ACI Journal Proceedings 53 (2), 29–58.

Ghali, A., Sargious, M.A., Huizer, A., 1974. Vertical prestressing of flat plates around columns, Shear in Reinforced Concrete. ACI Special Publication SP-42 2, 905–920.

Harajli, M.H., Soudki, K.A., 2003. Shear strengthening of interior slab-column connections using fiber reinforced polymer sheets. Journal of Composites for Construction, ASCE 7 (2), 145–153.

ISIS Canada, Strengthening reinforced concrete structures with externally-bonded fiber reinforced polymers, Design manual No. 4, Manitoba, Canada, (2001).

Marzouk, H., Jiang, D., 2007. Experimental investigation on shear enhancement types for high-strength concrete plates. ACI Structural Journal 94 (1), 49–58.

Miller, B., Nanni, A., 1999. Bond between carbon-fiber reinforced polymer sheets and concrete. In: Bank, L.C. (Ed.), Proceedings of the ASCE 5th Materials Congress. ASCE, Reston, VA, pp. 240–247.

Mowrer, R.D., Vanderbilt, M.D., 1967. Shear strength of light-weight aggregate reinforced concrete flat plates. ACI Journal Proceedings 64 (11), 722–729.

Ospina, C.E., Alexandre, S.D.B., Cheng, J.J.R., 2001. Behavior of concrete slabs with fiber-reinforced polymer reinforcement, Structural Engineering Report No. 242, Department of Civil and Environmental Engineering, University of Alberta, Alberta, Canada.

Sharaf, M.H., Soudki, K.A., Van Dusen, M., 2006. CFRP strengthening for punching shear of interior slab-column connections. Journal of Composites for Construction, ASCE 10 (5), 410–418.

Tan, K.H., 1996. Punching shear strength of RC slabs bonded with FRP systems, Proceedings of the 2nd International Conference on Advanced Composite Materials in Bridges and Structures, Montreal, Canada, pp. 387–394.

Zhang, J.W., Teng, J.G., Wong, Y.L., Lu, Z.T., 2001. Behavior of two-way RC slabs externally bonded with steel plate. Journal of Structural Engineering, ASCE 127 (4), 390–397.